

# Inhibition as a determinant of activity and criticality in dynamical networks

Joao Pinheiro Neto,<sup>1,2,\*</sup> Marcus A. M. de Aguiar,<sup>1</sup> José A. Brum,<sup>1</sup> and Stefan Bornholdt<sup>3</sup>

<sup>1</sup>*Institute of Physics “Gleb Wataghin”, University of Campinas, 13083-859, Campinas, Brazil*

<sup>2</sup>*Max Planck Institute for Dynamics and Self-Organization, 37077, Göttingen, Germany*

<sup>3</sup>*Institute for Theoretical Physics, University of Bremen, 28359, Bremen, Germany*

A certain degree of inhibition is a common trait of dynamical networks in nature, ranging from neuronal and biochemical networks, to social and technological networks. We study here the role of inhibition in a representative dynamical network model, characterizing the dynamics of random threshold networks with both excitatory and inhibitory links. Varying the fraction of excitatory links has a strong effect on the network’s population activity and its sensitivity to perturbation. The average degree  $K$ , known to have a strong effect on the dynamics when small, loses its influence on the dynamics as its value increases. Instead, the strength of inhibition is a determinant of dynamics and sensitivity here, allowing for criticality only in a specific corridor of inhibition. This criticality corridor requires that excitation dominates, while the balance region corresponds to maximum sensitivity to perturbation. We develop mean-field approximations of the population activity and sensitivity and find that the network dynamics is independent of degree distribution for high  $K$ . In a minimal model of an adaptive threshold network we demonstrate how the dynamics remains robust against changes in the topology. This adaptive model can be extended in order to generate networks with a controllable activity distribution and specific topologies.

## I. INTRODUCTION

Inhibition is a frequent factor in many real-world networks as nodes often have an excitatory, as well as an inhibitory effect on their neighbors. Actors in a social network may display affection or animosity towards each other, while genes may suppress the expression of others in a gene regulatory network. Notably, an estimate 20% of the neurons in the brain are inhibitory, and have a key role in regulating neuronal activity [1–4]. In model systems, dynamics with inhibition can generate more complex dynamics than their excitation-only counterparts [5].

Another common feature in real-world networks, also present in the brain, is a topology that evolves with time. In adaptive networks, feedback loops between network dynamics and topological evolution can drive the network towards different dynamical states. These can be critical points of a phase transition [6–8] or dynamical states not accessible to networks with standard (e.g. lattice or random) topologies [9–12]. To prevent changes in the topology from resulting in catastrophic failure of network function, it is important that the network dynamics be robust against such changes. The observation of avalanches of activity in cortical tissue, pointing towards a dynamical state near a phase transition [13–17], has also sparked renewed interest in models with phase transitions and mechanisms capable of controlling network evolution.

Random threshold networks (RTNs) have been used to model a vast array of phenomena [18–23], from neural networks [24] to gene regulatory networks [25, 26]. While RTNs have been extensively studied, in most models the links  $w_{ij}$  between nodes are either always excitatory ( $w_{ij} > 0$ ) or  $w_{ij} = \pm 1$  with equal probability. In the

following we generalize the RTN model to a varying balance between excitatory and inhibitory links in order to obtain insights into how inhibition may affect real-world networks. We use both network simulations (Sec. II) and analytic methods (Sec. III), and focus on the conditions for criticality and how we can control the network’s activity and dynamical sensitivity. We also study its robustness to topological evolution, and how, by evolving the topology, a higher degree of control of the dynamics is obtained.

## II. DYNAMICS OF RTNS WITH INHIBITION

### A. Model definition

Consider a directed network with  $n$  randomly connected nodes and average degree  $K$ . A weight  $w_{ij} = \pm 1$  is assigned to each existing link from node  $j$  to node  $i$ . The dynamical state of each node is represented by a Boolean variable. The state  $\sigma_i(t+1)$  of node  $i$  at time  $t+1$  is given by

$$\sigma_i(t+1) = \begin{cases} 1 & , \text{ if } \sum_{j=1}^n w_{ij}\sigma_j(t) > h \\ 0 & , \text{ if } \sum_{j=1}^n w_{ij}\sigma_j(t) \leq h \end{cases} \quad (1)$$

where  $h$  is a threshold parameter. The network collective state is measured by the fraction of active nodes,

$$A(t) = \frac{1}{n} \sum_i \sigma_i(t) \quad (2)$$

The dynamics is initiated by randomly choosing a fraction of the nodes to be activated at  $t = 0$ ,  $A(0)$ . We need a set of parameters to characterize the relevant topological properties of the network. These are the average degree  $K$  of the network, and the fraction of positive links

\* joaoxp@gmail.com

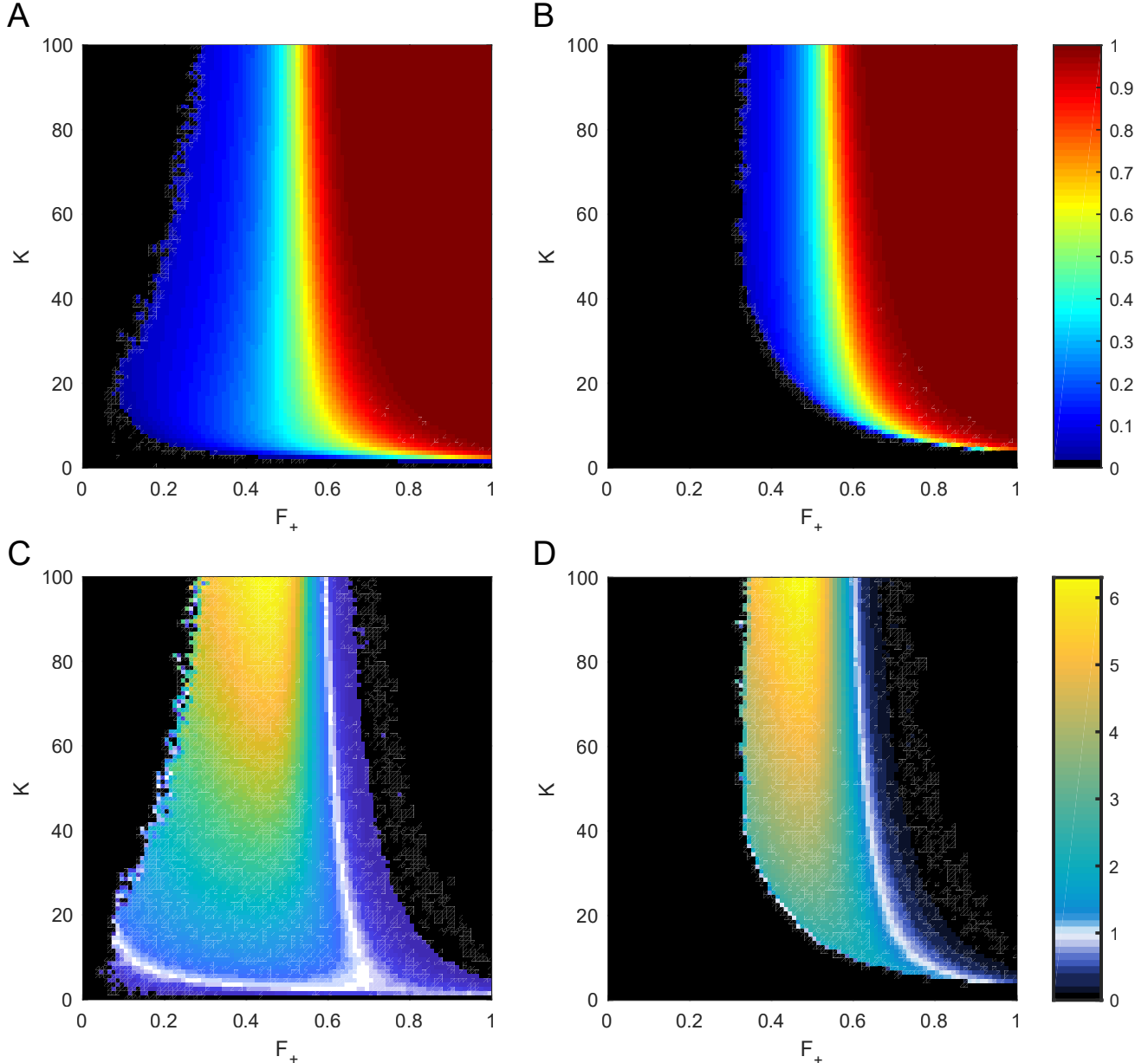


**Figure 1. Parameter space of the dynamics as a function of  $K$  and  $F_+$ .** **A.** Stable activity  $A_\infty$  for a threshold of  $h = 0$ . **B.** Same as (A) for  $h = 1$ . **C.** Sensitivity  $\lambda$  for  $h = 0$ . The white region corresponds to networks near criticality ( $\lambda = 1$ ). **D.** Same as (C) for  $h = 1$ . Balance ( $F_+ \approx 0.5$ ) results in maximum sensitivity, while criticality requires more excitation ( $F_+ > 0.5$ ) for high  $K$ . Other parameters are  $n = 10^3$  and  $A(0) = 0.9$ , and each point is the average of  $10^2$  simulations.

$F_+$ . The link weights  $w_{ij} = \pm 1$  are distributed randomly in the network, with the constraint that the total fraction of positive links is  $F_+$ . Unless otherwise stated, the underlying topology is that of a directed Erdős–Rényi (ER) network. As we will see, properties such as degree distribution are not critical in the high connectivity regime.

Several variants for the RTNs are possible. Some works in the literature add a self-regulating state [18, 22] to Eq. 1 given by  $\sigma_i(t+1) = \sigma_i(t)$  if  $\sum_{j=1}^n w_{ij}\sigma_j(t) = h$ . This new condition can drastically change the dynamics by adding long-term temporal correlations between the node

states. Note that for non-integer  $h$  (and  $w_{ij} = \pm 1$ ) this state is not possible, and the model is equivalent to ours. Our RTN definition with threshold  $h = 1$  is equivalent to the “biological” RTN variant as defined in [27], particularly suited for simulating genetic networks. Another possibility is to update the node states asynchronously [23] or use other forms of asynchronicity. In order to focus on the effect of  $F_+$  in ensembles of random networks, we will use the simpler and most common case where all nodes are updated in parallel according to Eq. 1.

## B. Parameter space

Since the dynamics is deterministic it must eventually arrive at an attractor. This can be a limit circle of  $A(t)$ , with  $A(t + \tau) = A(t)$  for some  $\tau$ , or a fixed point  $A_\infty$ , with  $A_\infty = A(t \rightarrow \infty)$ . The value  $A_\infty = 0$  is always a fixed point of the dynamics, since  $\sigma_i = 0$  for all  $i$  is an absorbing state. Szejka et al. [22] showed that for the specific case of  $F_+ = 0.5$  another stable fixed point  $A_\infty > 0$  can emerge depending on the relationship between  $K$  and  $h$ .

We ran numerical simulations in order to obtain  $A_\infty$  for the entire range  $0 < F_+ < 1$ . In Fig. 1A,B we plot the fixed point  $A_\infty$  in the parameter space  $A_\infty = A_\infty(F_+, K)$  for fixed thresholds  $h \in \{0, 1\}$ . We observe a much richer dynamics than in the  $F_+ = 0.5$  and  $F_+ = 1$  cases. Intuitively,  $A_\infty$  increases with  $F_+$ . However, the interesting aspect is that  $A_\infty$  can have a value on a large range, with the crucial parameter being  $F_+$ . The dependence on  $K \in [10, 100]$  is weaker, with the wider range of  $F_+$  with non-frozen dynamics (i.e.,  $A_\infty \neq 0$  and 1) happening for lower  $K$ . A critical degree  $K_C$  is necessary for  $A_\infty > 0$ , however. As  $K$  increases, the non-frozen dynamics becomes more centered around  $F_+ = 0.5$ , and in the  $K \rightarrow \infty$  limit only happens for  $A_\infty(0.5, K \rightarrow \infty) = 0.5$ . The convergence is slow, however. As the threshold  $h$  increases, the region in the  $(F_+, K)$  parameter space with non-frozen dynamics decreases. It is important to note that the transition from  $A_\infty = 0$  to  $A_\infty > 0$  is not a continuous transition. Very low activity network states can in principle happen, but they have a high probability of going to the absorbing state  $A(t) = 0$  (see Appendix A). Thus, in practice a finite network has a minimum stable activity  $A_\infty^C$  that it can sustain, which increases with larger  $h$ . In Sec. II C we explore  $A_\infty^C$  and other observables that define the dynamic range of RTNs.

Another important observable of RTNs is the network sensitivity  $\lambda$ . The sensitivity is defined as the number of perturbed states at time  $t + 1$  after changing the state of one node at time  $t$ , averaged over an ensemble of network states [18, 22]. For memoryless network dynamics this is enough to determine how a perturbation will spread over long timescales. If  $\lambda > 1$ , the network is chaotic and a perturbation will spread and take over the network. If  $\lambda < 1$ , the network is ordered and a perturbation will quickly die out. Finally, if  $\lambda = 1$ , the network is critical and a perturbation will take a long time to disappear without dominating the dynamics. In Figs. 1C,D we show the parameter space of  $\lambda$  as a function of  $F_+$  and  $K$  for  $h \in \{0, 1\}$ . In general,  $\lambda$  increases with  $K$  and is highest for networks with  $F_+ \approx 0.5$ .

Of particular interest are the regions of criticality where  $\lambda \approx 1$ . In Fig. 1C the near-horizontal white line corresponds to the well known critical point of discrete dynamical networks for a small critical value of  $K$  that only slightly depends on the, otherwise nearly arbitrary, degree of inhibition. A main observation of our paper

is the second, almost vertical, white line, indicating a second region of criticality for almost arbitrary and also high values of  $K$ , given that the fraction of positive links  $F_+$  lies within a narrow, well defined region. Here, the critical state requires  $\langle F_+ \rangle > 0.5$ , asymptotically approaching the balanced state ( $F_+ = 0.5$ ) in the  $K \rightarrow \infty$  limit. Nevertheless, well-connected finite-sized networks require more excitation than inhibition to attain criticality. Note also that, while criticality requires  $\langle F_+ \rangle > 0.5$ ,  $\langle F_+ \rangle \approx 0.5$  results in maximum sensitivity to perturbations (supercriticality).

Comparing the activity and sensitivity plots of Fig 1, we observe that the critical case is in general possible for a narrow region in connectivity  $K$  with relatively low activity, and a broad range of  $K$  at a higher activity level (see also Fig. 5B). This latter case, interestingly, combines conditions which are relevant for information processing networks: an intermediate activity level and a critical level of sensitivity. That this is closely correlated to a narrow range of inhibition in our RTN model may have implications for similar relationships in natural networks, as in the case of inhibition in the brain.

## C. Dynamic range of RTNs

Different combinations of topological and dynamical parameters can yield different values of  $A_\infty$ . With fixed  $h$  and  $K$  there is a critical  $F_+^C = F_+^C(K)$  required for  $A_\infty > 0$ , and the corresponding minimum activity  $A_\infty^C = A_\infty(F_+^C)$ . There is also a critical degree  $K^C = K^C(h)$ , which is the minimum connectivity required for  $A_\infty > 0$  with  $F_+ = 1$ . All of these quantities place boundaries on the activity of RTNs. If  $K < K_C$ , or  $F < F_+^C$ , no activity can be maintained by the network. More importantly,  $A_\infty^C$  is the minimum activity the network can maintain, and the knowledge of it is necessary for using Eq. 9 to generate RTNs with desired activity. In Fig. 2 we show  $A_\infty^C$ ,  $F_+^C$  and  $K_C$  (inset) for  $0 \leq h < 6$ . While  $A_\infty^C$  is low for low  $h$ , it can be quite high for high  $h$ . We obtain  $A_\infty^C = 0.51$  for  $K = 100$  and  $h = 6$ , meaning more than half of the network must be active in order for it to maintain activity with any  $F_+$ .

It is interesting to explore the range of values  $A_\infty$  can take by varying one parameter, as complete control of all parameters may not be feasible in certain situations. Lets us define the non-frozen range  $\Delta F_+$  of  $A_\infty$  as  $\Delta F_+ = F_2(K, h) - F_1(K, h)$ , where  $F_2$  is the highest and  $F_1$  the lowest  $F_+$  that produces non-frozen dynamics ( $0 < A_\infty < 1$ ) for a certain set of  $(K, h)$ . If there is no  $0 < A_\infty < 1$  possible we set  $\Delta F_+ = 0$ . In Fig. 2C we show  $\Delta F_+$ . As we increase both  $K$  and  $h$  the range  $\Delta F_+$  decreases, meaning the non-frozen dynamics gets compressed into a smaller range of values of  $F_+$ . The dynamic range  $\Delta A_\infty$  (i.e., the range of  $A_\infty$  the network can have by varying  $F_+$ ) is given by  $\Delta A_\infty = 1 - A_\infty^C$ . As  $K$  increases  $A_\infty^C$  decreases, with the exception of  $h = 0$  and low  $K$ . This means that in order to maintain a high dynamic range it

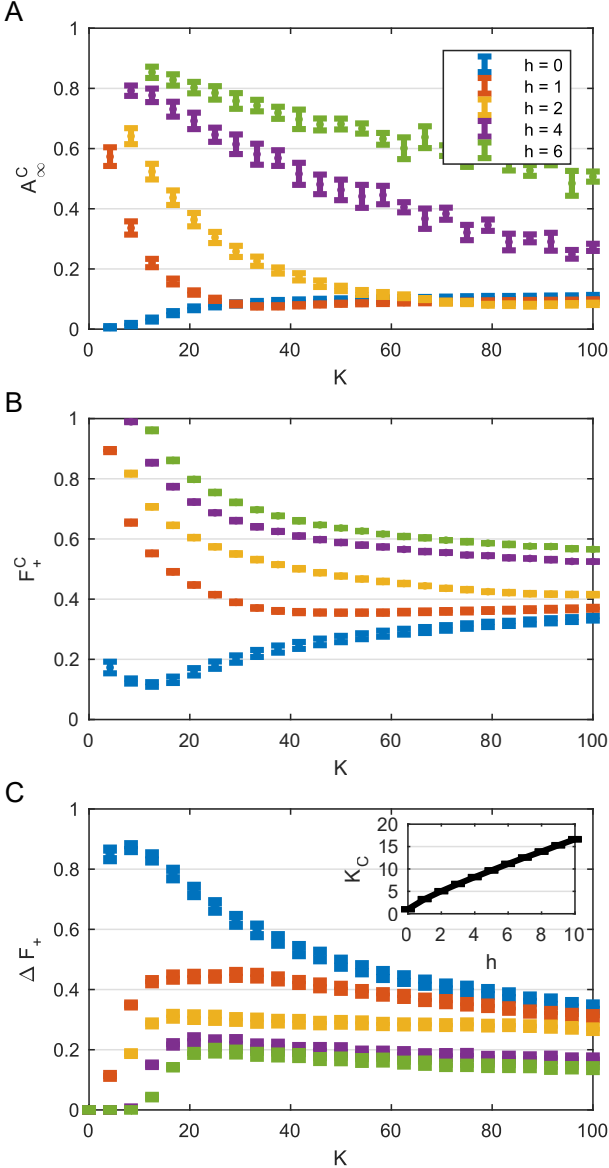


**Figure 2. Dynamic range as a function of the average degree  $K$  for  $0 \leq h \leq 6$**  **A.** Minimum stable activity  $A_\infty^C$  that an RTN can sustain. **B.** Critical  $F_+^C$  needed for the network to sustain activity. **C.** Non-frozen range  $\Delta F_+$  where the network produces non-frozen dynamics  $0 < A_\infty < 1$ . Inset: Minimum degree  $K_C$  needed for sustained activity. Parameters are  $n = 10^3$  and  $A(0) = 0.95$ , and each point is the average of  $10^2$  simulations. The color code is the same for all figures.

is advantageous for the network to be highly connected.

#### D. Adaptive networks with threshold dynamics

It is interesting to study how the RTN dynamics deals with an evolving topology. As we will see in Sec. III, the dynamics is fairly independent on the precise net-

work topology (Fig. 4C), making it a good candidate for a system that must be stable under changes to the topology. In the brain, during development a massive pruning process removes a large portion of the neuronal synapses [28]. Inspired by this, we study how a simple link-removal adaptation rule can shape the dynamics of the network.

The algorithm consists of removing an excitatory in-link of node  $i$  if its average activity  $\bar{A}_i$  is  $\bar{A}_i \geq \alpha$ , and removing an inhibitory in-link otherwise. While it can be expected that the algorithm can drive the individual node activity towards  $\alpha$ , it is not obvious whether it preserves the RTN dynamics or drives it towards a chaotic state. The algorithm, and its implications, are described in more detail in Appendix B.

Our simple algorithm consistently drives the global, stable activity to  $A_\infty \rightarrow \alpha$ . (Fig. 3A) for very different  $\alpha$  and initial fraction  $F_+^0$  of excitatory links. Thus, it can be used to evolve a network with thresholding dynamics towards a certain activity level with only local information. A natural extension is to allow different parameters  $\alpha_i$  for each node. In Fig. 3B we divide the  $n = 10^3$  nodes into 3 groups with  $\alpha \in \{0.1, 0.5, 0.9\}$ , and show that the algorithm can lead to the co-existence of groups with very different activity rates within the same network.

The adaptive algorithm allows us to control not only  $A_\infty$ , but the node activity distribution  $p_A(\bar{A}_i)$ . This is particularly useful because the RTN dynamics with a random (ER) network results in a bimodal  $p_A(\bar{A}_i)$ . In other words, a high number of nodes is either always on ( $A_i = 1$ ) or always off ( $A_i = 0$ ), which can be undesirable. By evolving the network, we can obtain more a Gaussian activity distribution. This is shown in Fig. 3C, where an RTN with  $F_+ = 0.54$  and an evolved network with  $\alpha = 0.75$  have the same  $A_\infty = 0.74$ , but very different  $p_A(\bar{A}_i)$ . The  $p_A(\bar{A}_i)$  of the evolved network from Fig. 3B displays three peaks centered around each of the  $\alpha \in \{0.1, 0.5, 0.9\}$ . Thus, for large enough networks, this can in principle be used to obtain an arbitrary activity distribution  $p_A(\bar{A}_i)$  within the network.

### III. MEAN-FIELD THEORY

#### A. Activity $A_\infty$

The annealed approximation was introduced by Derrida & Pomeau [29] and it is a useful tool to study the dynamics of RTNs. The idea behind it is to ignore temporal correlations between nodes, making each node independent. This is equivalent to shuffling the network links at each timestep. When we take into account the effect of  $F_+$ , the activity at time  $t + 1$  is given by

$$A(t+1) = \sum_{k=1}^{n-1} p_k \sum_{m=h+1}^k \binom{k}{m} A(t)^m (1 - A(t))^{k-m} P_+(m) \quad (3)$$

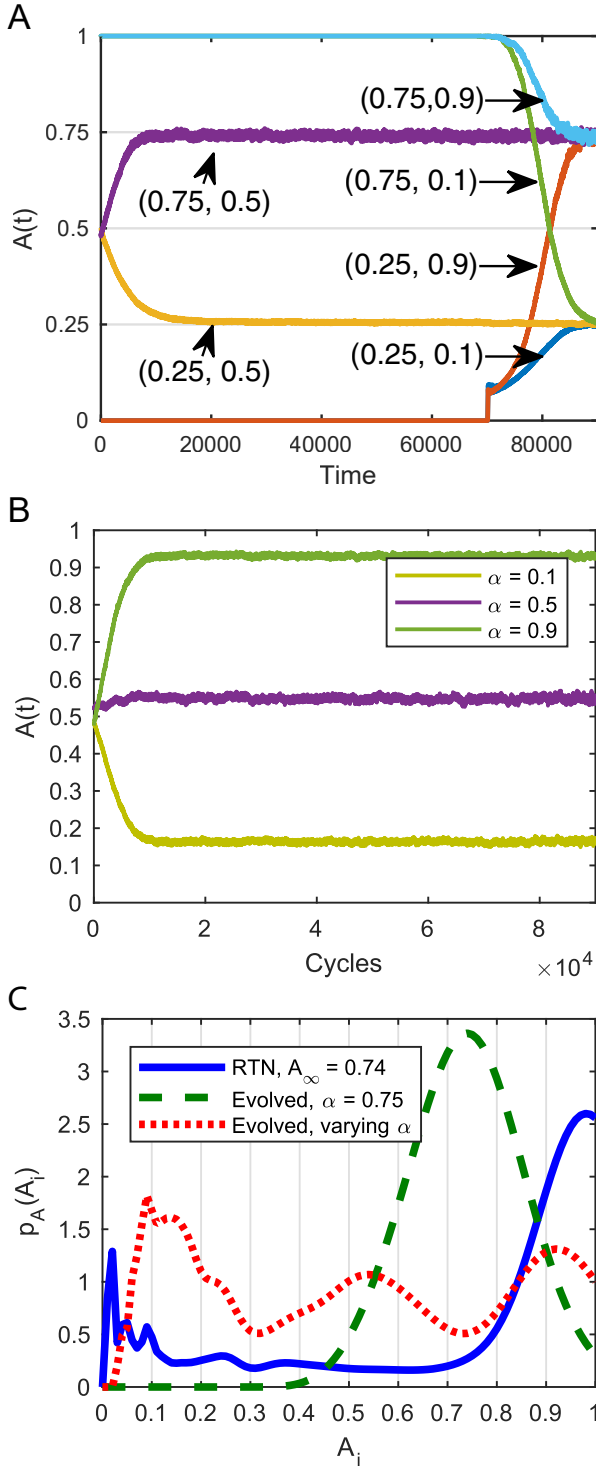


**Figure 3. Network activity with an adaptive algorithm.** **A.** Evolution with a single  $\alpha$  for the network. The arrows indicate the parameters  $(\alpha, F_+^0)$ . **B.** Evolution with multiple  $\alpha \in \{0.1, 0.5, 0.9\}$  within the same network. **C.** Activity distribution between nodes  $p_A(\bar{A}_i)$  for the RTN (full line) with  $F_+ = 0.54$  and  $A_\infty = 0.74$ , evolved network with  $\alpha = 0.75$  and  $F_+^0 = 0.5$  (dashed line) and the evolved network from (B) (dotted line). Other parameters are  $n = 10^3$ ,  $K = 10^2$  and  $h = 0$ .

where  $P_+(m)$  is given by

$$P_+(m) = \sum_{l=\lfloor \frac{m+h}{2} \rfloor + 1}^m \binom{m}{l} F_+^l (1 - F_+)^{m-l} \quad (4)$$

with  $p_K$  denoting the degree distribution of the network, and  $\lfloor x \rfloor$  the floor function of  $x$ . In principle, Eq. 3 can be solved graphically to yield  $A_\infty$ . It compares favorably with numerical simulations for the dynamics of RTNs without a self-regulating state [18]. An interesting feature of Eq. 3 is that it predicts more than two fixed points  $A_\infty$  for some cases. For instance, for  $K = 25$ ,  $h = 2$  and  $F_+ = 0.6$  with an ER topology the fixed points are  $A_\infty \in \{0, 0.10, 0.49\}$ . Nonetheless, we were unable to find more than one stable non-zero fixed point ( $A_\infty = 0.49$  in this case) in the explored parameter space.

The annealed approximation has some quirks, however. It demands the knowledge of the full degree distribution, which is not relevant in the high-degree regime (Fig. 4C). Care must also be taken when numerically evaluating it, as naively computing  $\binom{m}{l} F_+^l (1 - F_+)^{m-l}$  can lead to machine precision errors. More importantly, it does not easily tell us how to generate a network with a determined value of  $A_\infty$ . In this section we obtain a simplified version of Eq. 3 with the aim to facilitate its application to the study of RTNs.

Let us first look into Eq. 4, as  $P_+(m)$  is the most important term of Eq. 3. We can use the identity

$$I_p(n+1, N-n) = \sum_{i=n+1}^N \binom{N}{n} p^i (1-p)^{N-i} \quad (5)$$

to write  $P_+(m)$  in terms of the regularized incomplete beta function  $I_z(a, b)$ , which is defined for non-integer  $a$  and  $b$ . By approximating  $\lfloor x/2 \rfloor \approx x/2 - 1/4$ , we can write

$$P_+(m) = I_{F_+} \left( \frac{m+h+3/2}{2}, \frac{m-h+1/2}{2} \right) \quad (6)$$

As already mentioned, in the high-degree regime the influence of the degree distribution is small. We can then substitute the sum over  $p_K$  in Eq. 3 for the average degree  $K$ . If we assume that  $P_+(m)$  is a slow-varying function, we can remove it from the innermost sum in Eq. 3 and substitute  $m$  by its average value  $\bar{m} = KA_\infty$ . We can then write

$$A_\infty = \sum_{m=h+1}^K \left\{ \binom{K}{m} A_\infty^m (1 - A_\infty)^{K-m} \right\} P_+(KA_\infty) \quad (7)$$

For high degree  $K$ , we can approximate  $\sum_{m=h+1}^K \binom{K}{m} A_\infty^m (1 - A_\infty)^{K-m} \approx 1$ , and using Eq. 6 we write

$$A_\infty = I_{F_+} \left( \frac{KA_\infty + h + 3/2}{2}, \frac{KA_\infty - h + 1/2}{2} \right) \quad (8)$$

The usefulness of Eq. 8 lies in the fact that  $I_z(a, b)$  is a standard function in most algebra packages. Therefore, Eq. 8 can be quickly solved graphically or numerically with minimal effort. More importantly, the inverse of  $I_X(a, b) = Y$ ,  $I_Y^{-1}(a, b) = X$  is also a standard function. We can use it to write

$$F_+ = I_{A_\infty}^{-1} \left( \frac{KA_\infty + h + 3/2}{2}, \frac{KA_\infty - h + 1/2}{2} \right) \quad (9)$$

which gives us the necessary value for  $F_+$  to generate a RTN with degree  $K$  and activity  $A_\infty$ . This allows us to control the activity  $A_\infty$  of the network by manipulating the balance between excitatory and inhibitory links.

In Fig. 4 we compare the results from Eq. 9 (plotted with inverted axis) and numerical simulations. Our simplified approximation matches well the simulation results in most cases. However, it fails to capture the transition between  $A_\infty = 0$  and  $A_\infty > 0$ , producing a second low  $A_\infty$  fixed point that is not observed in Eq. 3. This is caused by our assumption that  $P_+(m)$  is slow-varying breaking down at the transition between  $A_\infty = 0$  and  $A_\infty > 0$ . Our simplification of  $p_k = \delta_{k,K}$  can also produce divergences for low  $K$  and high  $h$ , where the degree distribution of the network can significantly change  $A_\infty$ . This is evident in Figure 4C, where we compare  $A_\infty$  for networks with Erdős-Rényi (ER) and Barabási-Albert (BA) topologies [30, 31] and  $h = 2$ . As  $K$  increases, however, both converge to the same  $A_\infty$ . For  $h > 2$ , both ER and BA networks converge to the same  $A_\infty$  even with  $K = 10$  (not shown).

It is important to note that for high  $K$  the approximation fails in one direction: predicting  $A_\infty > 0$  for a network with  $A_\infty = 0$ . When the network has a non-zero  $A_\infty$  the results of our approximation are quite accurate to describe the fixed point activity of the network. Therefore, if we know that the network can maintain activity and is well-connected, we can use Eq. 8 and 9 to predict its properties. In other words, our approximation is applicable as long as  $A_\infty > A_\infty^C$ , which is shown in Fig. 2A.

## B. Sensitivity $\lambda$

The sensitivity of RTNs was studied in [18]. The model used, however, has long-term correlations resulting in a complicated mean-field approximation. In this section we propose a simpler mean-field approximation of  $\lambda$  for the dynamics defined in Eq. 1, and study its relationship to the network activity  $A_\infty$ .

The basic idea of the approximation is to look into the contribution of a node  $j$  in the input sum  $S_i(t) = \sum_k w_{ik}\sigma_k(t)$  of node  $i$ . Let us define the input sum of  $i$  at time  $t$  without considering  $j$  as  $S'_i = \sum_{k \neq j} w_{ij}\sigma_k(t)$ . For a threshold of  $h$ , a flip of  $\sigma_j(t)$  can only cause a flip of  $\sigma_i(t+1)$  if  $S'_i(t) = h$  or  $S'_i(t) = h+1$ . If  $P(m)$  is the probability of node  $i$  having  $m$  active neighbors

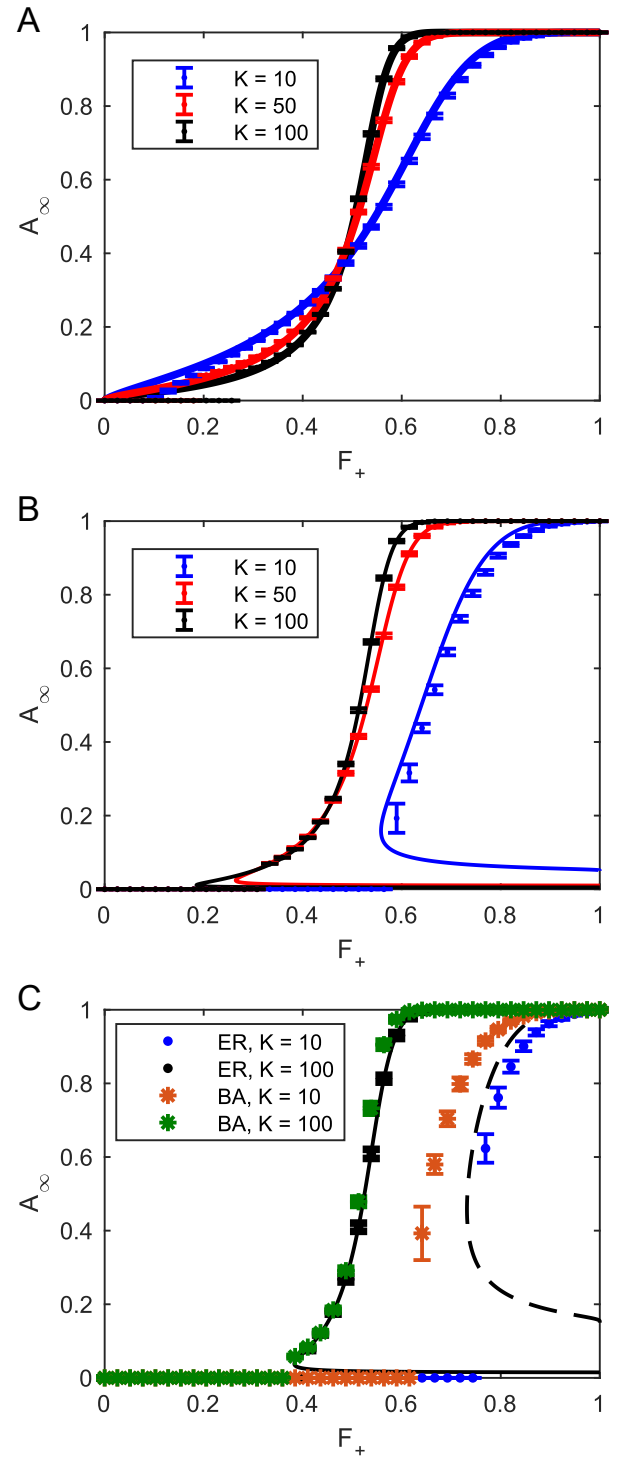
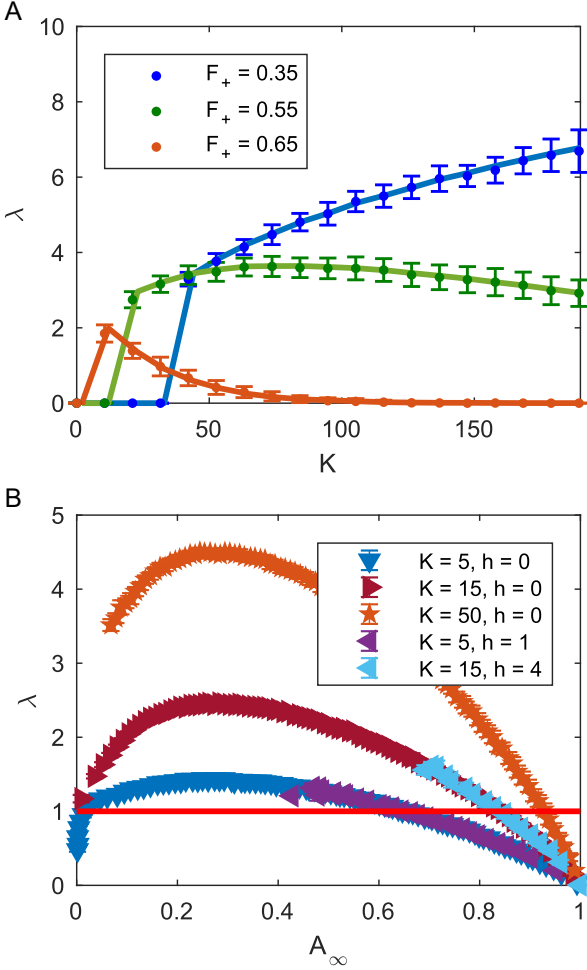


Figure 4. Comparison between simulations (points) and the mean-field approximation (lines) for  $A_\infty$ . **A.** Results for ER networks with  $h = 0$  and  $K \in \{10, 50, 100\}$ . **B.** Same as (A) for  $h = 1$ . **C.** Comparison for ER and BA networks with the approximation for  $K = 10$  (solid line) and  $K = 100$  (dashed line). Parameters are  $n = 10^3$  and  $A(0) = 0.95$ , and each point is the average of  $10^2$  simulations.



**Figure 5. Sensitivity  $\lambda$  of RTNs.** **A.** Comparison between simulations (points) and the mean-field approximation (lines) for  $h = 1$ . **B.** Relationship between  $A_\infty$  and  $\lambda$  for varying  $K$  and  $h$ . The red line corresponds to critical dynamics ( $\lambda = 1$ ). Parameters are  $n = 10^3$  and  $A(0) = 0.9$ , and each point is the average of  $10^2$  simulations.

between  $k - 1$  in-neighbors, the probability  $P_k(j, i)$  of node  $j$  inducing a flip on node  $i$  is given by

$$P_k(j, i) = \sum_{m=h}^{k-1} P(m) \left\{ P(S'_i = h) P_k(j, i | S'_i = h) + P(S'_i = h+1) P_k(j, i | S'_i = h+1) \right\} \quad (10)$$

where

$$P(m) = \binom{k-1}{m} A_\infty^m (1 - A_\infty)^{k-1-m} \quad (11)$$

For  $m$  active nodes  $S'_i = h$  is only possible if  $m + h$  is even and  $m \geq h$ . In this case we have

$$P(S'_i = h) = \binom{m}{(m+h)/2} F_+^{(m+h)/2} (1 - F_+)^{(m-h)/2} \quad (12)$$

Likewise,  $S'_i = h + 1$  is only possible if  $m + h$  is odd and  $m \geq h + 1$ . In this case

$$P(S'_i = h+1) = \binom{m}{m+h+1} F_+^{(m+h+1)/2} (1 - F_+)^{(m-h-1)/2} \quad (13)$$

If  $S'_i = h$ , node  $j$  can only alter the state of  $i$  if  $w_{ij} = +1$ . If  $S'_i = h + 1$  however, node  $j$  can flip  $i$  only if  $w_{ij} = -1$ . In other words,  $P_k(j, i | S'_i = h) = F_+$  and  $P_k(j, i | S'_i = h + 1) = 1 - F_+$ . Substituting Eq. 11-13 into Eq. 10, we have

$$P_k(j, i) = \sum_{m=h}^{k-1} \binom{k-1}{m} A^m (1 - A)^{K-1-m} \times F_+^{(m+h)/2} (1 - F_+)^{(m-h)/2} \gamma_h(m, F_+) \quad (14)$$

where

$$\gamma_h(m, F_+) = \begin{cases} \binom{m}{(m+h)/2} F_+ & , m + h \text{ even} \\ \binom{m}{(m+h+1)/2} \sqrt{F_+ (1 - F_+)} & , m + h \text{ odd} \end{cases} \quad (15)$$

The sensitivity  $\lambda$  is the mean value of  $P_k(j, i)$ :

$$\lambda = \sum_{k=1}^{n-1} p_k^{in} P_k(j, i) \quad (16)$$

where  $p_k^{in}$  denotes the in-degree distribution of the network. If we approximate  $p_k^{in} \rightarrow K$ , we have our final result

$$\lambda = K \sum_{m=h}^{K-1} \binom{K-1}{m} A_\infty^m (1 - A_\infty)^{K-1-m} \times F_+^{(m+h)/2} (1 - F_+)^{(m-h)/2} \gamma_h(m, F_+) \quad (17)$$

where  $\gamma_h(m, F_+)$  is given by Eq. 15. In Fig. 5A we compare Eq. 17 to simulation results for  $h = 1$ . Our approximation provides a good match to the results.

As both  $\lambda$  and  $A_\infty$  depend on the same set of parameters, they cannot be freely chosen. We can then use  $\lambda$  as a constraint on  $A_\infty$ . This can be done by numerically solving the coupled system made of Eq. 3 and Eq. 16. However, in the high  $K$  regime we can substitute Eq. 9 into Eq. 17 to obtain  $\lambda = \lambda(A_\infty, K, h)$ . In Fig. 5B we show the relationship between  $\lambda$  and  $A_\infty$  for varying  $K$  and  $h$ . The network is insensitive to perturbation for  $A_\infty = 0$  and  $1$ . Between these two extremes  $\lambda$  is a concave function of  $A_\infty$ , with higher  $K$  resulting in higher  $\lambda$ . While  $h$  creates regions with  $\lambda = 0$  (Fig. 2B), it does not significantly change the value of  $\lambda > 0$ . There exists a critical point ( $\lambda = 1$ ) for most  $K$  and  $h$  and high  $A_\infty$ . However, if  $K$  is low (and  $h$  is also low, to allow  $A_\infty > 0$ ) another critical point will appear with low  $A_\infty$ .

#### IV. DISCUSSION

At the core of our study is the idea that Random Threshold Networks are robust to changes in the topol-

ogy, and that their activity can be controlled by balancing excitation and inhibition. Here, we found a much richer dynamics for varying fractions of excitatory and inhibitory links than for the special case of equal balance ( $F_+ = 0.50$ ). The stable network activity covers a large and non-trivial range of values, and we find that network sensitivity and activity depend on the same factors, and cannot be freely chosen.

More importantly we find that, for well-connected networks, criticality requires an excess of excitatory connections, and is only possible in a narrow band of inhibition. Our model results pose interesting questions w.r.t. inhibition in the brain. GABAergic neurons *in vitro* are known to shift from having an excitatory to inhibitory effect during development [32]. In our model, the shift results in subcritical dynamics early on being a necessary step to reach criticality, which is compatible with results of avalanches of activity *in vitro* [33, 34]. Evidence points towards no GABA shift *in vivo*, however, with GABAergic neurons always being inhibitory [35, 36]. In this situation, our model predicts that a constant level of inhibition is required for criticality during network growth. This is compatible with the finding that the fraction of GABAergic neurons is constant during development *in vivo* [37]. Thus, our results on the influence of inhibition on the critical point possibly provide independent support for the hypothesis of a near-critical dynamics in cortical tissue.

Using a simple adaptive algorithm, we increased our control from the global average to the activity distribution within the network. The model can also be extended

in other ways in order to generate specific topologies. For instance, a link creation rule can be used to balance the link pruning, or link shuffling to maintain the degree distribution. The topological evolution rules can also be changed in order to control other properties of the network. Scale-free networks with controllable activity can in principle be generated both through growth [31] and pruning [38].

Overall our RTN model, using simple threshold units, is able to generate rich dynamics with a phase transition. It does not depend on details of the network topology, and has both inhibitory interactions and stable, ceaseless dynamics. This can make the RTN an interesting minimal model to explore mechanisms of neural dynamics, as the brain has inhibition, an evolving topology and a dynamics with input integration and thresholding.

## ACKNOWLEDGMENTS

JPN thanks the financial support of the São Paulo Research Foundation (FAPESP) under grants 2012/18550-4 and 2013/15683-6, and of the Brazilian National Council for Scientific and Technological Development (CNPq) under grant 206891/2014-8. MAM thanks the financial support of FAPESP under grants 2016/06054-3 and 2016/01343-7, and CNPq under grant 302049/2015-0. JAB thanks the financial support of FAPESP under grant 2016/04783-8.

- 
- [1] György Buzsáki, Kai Kaila, and Marcus Raichle. Inhibition and Brain Work. *Neuron*, 56(5):771–783, dec 2007.
  - [2] Henry Markram, Maria Toledo-Rodriguez, Yun Wang, Anirudh Gupta, Gilad Silberberg, and Caizhi Wu. Interneurons of the neocortical inhibitory system. *Nat. Rev. Neurosci.*, 5(10):793–807, oct 2004.
  - [3] Jeffry S Isaacson and Massimo Scanziani. How inhibition shapes cortical activity. *Neuron*, 72(2):231–243, oct 2011.
  - [4] Taro Toyoizumi, Hiroyuki Miyamoto, Yoko Yazaki-Sugiyama, Nafiseh Atapour, Takao K. K. K Hensch, and Kenneth D. D. D Miller. A Theory of the Transition to Critical Period Plasticity: Inhibition Selectively Suppresses Spontaneous Activity. *Neuron*, 80(1):51–63, 2013.
  - [5] Daniel B. Larremore, Woodrow L. Shew, Edward Ott, Francesco Sorrentino, and Juan G. Restrepo. Inhibition Causes Ceaseless Dynamics in Networks of Excitable Nodes. *Phys. Rev. Lett.*, 112(13):138103, apr 2014.
  - [6] Per Bak, Chao Tang, and Kurt Wiesenfeld. Self-organized criticality: An explanation of the 1/f noise. *Phys. Rev. Lett.*, 59(4):381–384, jul 1987.
  - [7] Stefan Bornholdt and Thimo Rohlfs. Topological evolution of dynamical networks: global criticality from local dynamics. *Phys. Rev. Lett.*, 84(26 Pt 1):6114–6117, jun 2000.
  - [8] Matthias Rybarsch and Stefan Bornholdt. Avalanches in self-organized critical neural networks: a minimal model for the neural SOC universality class. *PLoS One*, 9(4):e93090, jan 2014.
  - [9] Thilo Gross and Hiroki Sayama, editors. *Adaptive Networks. Understanding Complex Systems*. Springer Berlin Heidelberg, Berlin, Heidelberg, 2009.
  - [10] Thilo Gross and Bernd Blasius. Adaptive coevolutionary networks: a review. *J. R. Soc. Interface*, 5(October 2007):259–271, mar 2008.
  - [11] Thilo Gross, Carlos J Dommar D’Lima, and Bernd Blasius. Epidemic dynamics on an adaptive network. *Phys. Rev. Lett.*, 96(20):208701, may 2006.
  - [12] Takaaki Aoki and Toshio Aoyagi. Scale-Free Structures Emerging from Co-evolution of a Network and the Distribution of a Diffusive Resource on it. *Phys. Rev. Lett.*, 109(20):208702, nov 2012.
  - [13] John M Beggs and Dietmar Plenz. Neuronal avalanches in neocortical circuits. *J. Neurosci.*, 23(35):11167–77, dec 2003.
  - [14] Nir Friedman, Shinya Ito, Braden A W Brinkman, Masanori Shimono, R. E Lee Deville, Karin A. Dahmen, John M. Beggs, and Thomas C. Butler. Universal critical dynamics in high resolution neuronal avalanche data. *Phys. Rev. Lett.*, 108(20):1–5, 2012.
  - [15] Dietmar Plenz and Ernst Niebur, editors. *Criticality in Neural Systems*. Wiley-VCH Verlag GmbH & Co. KGaA, Weinheim, Germany, apr 2014.

- [16] Viola Priesemann, Michael Wibral, Mario Valderrama, Robert Pröpper, Michel Le Van Quyen, Theo Geisel, Jochen Triesch, Danko Nikolić, and Matthias H J Munk. Spike avalanches in vivo suggest a driven, slightly subcritical brain state. *Front. Syst. Neurosci.*, 8(June):108, 2014.
- [17] Jens Wilting and Viola Priesemann. Branching into the Unknown: Inferring collective dynamical states from subsampled systems. 2016.
- [18] Jorge G. T. Zañudo, Maximino Aldana, and Gustavo Martínez-Mekler. Boolean Threshold Networks: Virtues and Limitations for Biological Modeling. In Samuli Niiranen and Andre Ribeiro, editors, *Inf. Process. Biol. Syst.*, volume 11 of *Intelligent Systems Reference Library*, pages 113–135. Springer Berlin Heidelberg, Berlin, Heidelberg, 2011.
- [19] M Andrecut, D Foster, H Carteret, and S a Kauffman. Maximal information transfer and behavior diversity in Random Threshold Networks. *J. Comput. Biol.*, 16(7):909–916, jul 2009.
- [20] Thimo Rohlff and Stefan Bornholdt. Criticality in random threshold networks: annealed approximation and beyond. *Phys. A Stat. Mech. its Appl.*, 310(1-2):245–259, jul 2002.
- [21] Thimo Rohlff. Critical line in random-threshold networks with inhomogeneous thresholds. *Phys. Rev. E*, 78(6):66118, dec 2008.
- [22] Agnes Szejka, Tamara Mihaljev, and Barbara Drossel. The phase diagram of random threshold networks. *New J. Phys.*, 10(6):063009, jun 2008.
- [23] Rui-Sheng Wang and Réka Albert. Effects of community structure on the dynamics of random threshold networks. *Phys. Rev. E*, 87(1):012810, jan 2013.
- [24] Warren S. McCulloch and Walter Pitts. A logical calculus of the ideas immanent in nervous activity. *Bull. Math. Biophys.*, 5(4):115–133, dec 1943.
- [25] Maria Davidich and Stefan Bornholdt. Boolean network model predicts cell cycle sequence of fission yeast. *PLoS One*, 3(2):e1672, jan 2008.
- [26] Fangting Li, Tao Long, Ying Lu, Qi Ouyang, and Chao Tang. The yeast cell-cycle network is robustly designed. *Proc. Natl. Acad. Sci. U. S. A.*, 101(14):4781–4786, apr 2004.
- [27] Matthias Rybarsch and Stefan Bornholdt. Binary threshold networks as a natural null model for biological networks. *Phys. Rev. E - Stat. Nonlinear, Soft Matter Phys.*, 86(2):1–6, 2012.
- [28] P R Huttenlocher and C de Courten. The development of synapses in striate cortex of man. *Hum. Neurobiol.*, 6(1):1–9, 1987.
- [29] B Derrida and Y Pomeau. Random Networks of Automata: A Simple Annealed Approximation. *Europhys. Lett.*, 1(2):45–49, jan 1986.
- [30] Paul Erdős and Alfred Rényi. On random graphs. *Publ. Math.*, 6(1):290–297, nov 1959.
- [31] Albert-László Barabási and Réka Albert. Emergence of Scaling in Random Networks. *Science (80-)*, 286(5439):509–512, oct 1999.
- [32] Yeheskel Ben-Ari. Excitatory actions of GABA during development: The nature of the nurture. *Nat. Rev. Neurosci.*, 3(9):728–739, 2002.
- [33] V. Pasquale, P. Massobrio, L. L. Bologna, M. Chiappalone, and S. Martinoia. Self-organization and neuronal avalanches in networks of dissociated cortical neurons. *Neuroscience*, 153(4):1354–1369, 2008.
- [34] A Levina and V Priesemann. Subsampling scaling. *Nat. Commun.*, 8(May):15140, may 2017.
- [35] Knut Kirmse, Michael Kummer, Yury Kovalchuk, Otto W. Witte, Olga Garaschuk, and Knut Holthoff. GABA depolarizes immature neurons and inhibits network activity in the neonatal neocortex in vivo. *Nat. Commun.*, 6:1–13, 2015.
- [36] Guzel Valeeva, Thomas Tressard, Marat Mukhtarov, Agnes Baude, and Rustem Khazipov. An Optogenetic Approach for Investigation of Excitatory and Inhibitory Network GABA Actions in Mice Expressing Channelrhodopsin-2 in GABAergic Neurons. *J. Neurosci.*, 36(22):5961–5973, 2016.
- [37] S. Sahara, Y. Yanagawa, D. D. M. O’Leary, and C. F. Stevens. The Fraction of Cortical GABAergic Neurons Is Constant from Near the Start of Cortical Neurogenesis to Adulthood. *J. Neurosci.*, 32(14):4755–4761, 2012.
- [38] Christian M Schneider, L. de Arcangelis, and H. J. Herrmann. Scale-free networks by preferential depletion. *EPL (Europhysics Lett.)*, 95(1):16005, jul 2011.

## Appendix A: Dependence on $A(0)$

Which fixed point ( $A_\infty = 0$  or  $A_\infty > 0$  if it exists) the dynamics stays at depends on the input  $A(0)$  used to activate the network. A critical input  $A_0^C$  is needed for ceaseless dynamics, below which the network quickly goes to  $A_\infty = 0$ . This is exemplified in Fig. 6A, where the dynamics dies out for  $A(0) = 0.01$  but not for  $A(0) \geq 0.02$ . The value of  $A_0^C$  can be obtained numerically from a mean-field approximation (Sec. IIIA), corresponding to the  $n \rightarrow \infty$  case. For any realization of the dynamics, however, there is a probability of it dying out even if  $A(0) > A_0^C$ . This probability depends chiefly on the value of  $A(t)$ , so if  $A_\infty$  is high the dynamics is only likely to die at the beginning and with a low  $A(0)$ . The time it takes for the dynamics to reach  $A_\infty$  depends predominantly on  $A(0)$ , but also on factors such as the degree distribution  $p_K$  of the network and  $\lambda$ . In Fig. 6B we show the dependency of the probability  $P_{\text{death}}$  of extinction (i.e.  $A(t) = 0$ ) on  $A(0)$  as a function of  $n$ . As  $n \rightarrow \infty$ ,  $P_{\text{death}}$  resembles a step function. In order to sidestep this issue, in the main text we always activate the network with a high  $A(0) = 0.90$  or  $A(0) = 0.95$ .

## Appendix B: Adaptive algorithm

Here we describe in more detail the adaptive algorithm used in Sec. IID. The average activity of node  $i$  is defined as  $\bar{A}_i = \sum_{t=0}^{t=\tau} \sigma_i(t)/\tau$ , where  $\tau = 10$  defines a moving average. In the adaptive process, each  $\bar{A}_i$  is compared to a parameter  $\alpha_i$  and change its connectivity according to a certain set of rules. The important question is then which set of rules, combined with a specific distribution of  $\bar{A}_i$ , can produce a certain topology and network activity. In other words, the problem amounts to the exploration of the class of adaptive threshold networks with local, activity-based topological evolution. Here we follow the simple algorithm:

1. If  $A(t) = 0$  activate a fraction  $A_0$  of the network nodes.
2. Run the dynamics of Eq. 1 for  $\tau$  timesteps, and choose a random node  $i$ .
3. If  $\bar{A}_i > \alpha_i$ , remove a random positive in-link of  $i$ . Otherwise remove a random negative in-link. If there is no suitable link for removal, choose another  $i$ .
4. Iterate from step 1.

The above algorithm can only be run a finite number of cycles. Since a single link is removed after each cycle, we can set the average degree  $K$  of the evolved network by running the algorithm  $\tau_{\text{cycle}} = n(K_0 - K)$  cycles, where  $K_0$  is the average degree of the initial network.

The choice of  $\tau$  is not important, since  $A(t)$  stabilizes

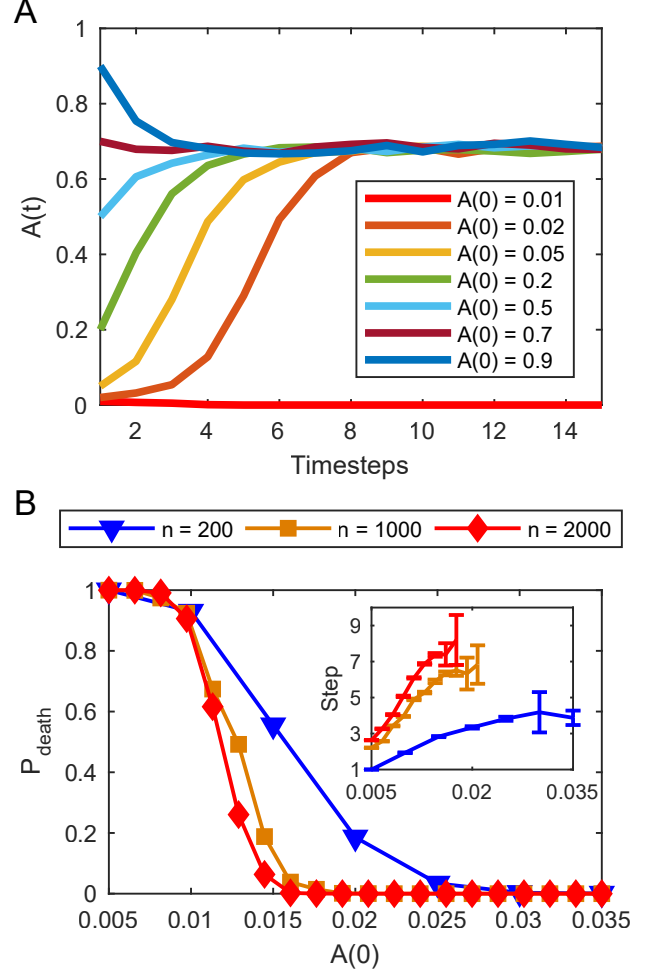


Figure 6. **Effect of  $A(0)$  on the dynamics.** **A.** Effect of different  $A(0)$  on a network with  $n = 1000$ . **B.** Probability  $P_{\text{death}}$  of the dynamics dying out for  $n \in \{200, 1000, 2000\}$ . Inset: Average step of death for the simulations that ended in  $A = 0$ . Each point is an average from 20 networks and  $10^3$  simulations each. Other parameters are  $K = 25$ ,  $F_+ = 0.6$  and  $h = 1$  for both cases.

quickly. This leaves us with only two evolutionary parameters,  $\alpha$  and  $\tau_{\text{cycle}} = n(K_0 - K)$ . If we start from a fully connected network, the in-degree distribution  $p_k^{\text{in}}$  of the evolved network is given by

$$p_k^{\text{in}} = \binom{n(n-1-K)}{n-1-k} \left(\frac{1}{n}\right)^{n-1-k} \left(1 - \frac{1}{n}\right)^{n(n-1-K)-(n-1-k)} \quad (\text{B1})$$

and the out-degree distribution  $p_k^{\text{out}}$  is given by

$$p_k^{\text{out}} = \binom{n}{k} \left(\frac{K}{n-1}\right)^k \left(1 - \frac{K}{n-1}\right)^{n-k} \quad (\text{B2})$$

While both distributions are binomial, the in-degree distribution is wider than the out-degree.